



SYMPOSIUM

Comparative study of snake lateral undulation kinematics in model heterogeneous terrain

Perrin E. Schiebel , Alex M. Hubbard and Daniel I. Goldman¹

School of Physics, Georgia Institute of Technology, Atlanta, GA, USA

From the symposium “Long Limbless Locomotors: The Mechanics and Biology of Elongate, Limbless Vertebrate Locomotion” presented at the annual meeting of the Society for Integrative and Comparative Biology, January 3–7, 2020 at Austin, Texas.

¹E-mail: daniel.goldman@physics.gatech.edu

Synopsis Terrestrial organisms that use traveling waves to locomote must leverage heterogeneities to overcome drag on the elongate body. While previous studies illuminated how habitat generalist snakes self-deform to use rigid obstacles in the surroundings, control strategies for multi-component terrain are largely unknown. We compared the sand-specialist *Chionactis occipitalis* to a habitat generalist, *Pantherophis guttatus*, navigating a model terrestrial terrain—rigid post arrays on a low-friction substrate. We found the waveshapes used by the generalist were more variable than the specialist. Principal component analysis revealed that while the specialized sand-swimming waveform was always present on *C. occipitalis*, the generalist did not have a similarly pervasive low-dimensional waveshape. We expected the generalist to thus outperform the specialist in the arrays, but body slip of both species was comparable on level ground and in all trials the snakes successfully traversed the arena. When we further challenged the snakes to ascend an inclined lattice, the sand-specialist had difficulty maintaining contact with the obstacles and was unable to progress up the steepest inclines in the largest lattice spacings. Our results suggest that species adapted to different habitats use different control modalities—the specialist is primarily controlling its kinematics to achieve a target shape while, consistent with previous research, the generalist is using force control and self-deforms in response to terrain contacts. While both strategies allowed progress on the uninclined low-friction terrain with posts, the more variable waveshapes of the generalist may be necessary when faced with more challenging locomotor tasks like climbing inclines.

Introduction

Despite the apparent specialization of limblessness, animals like snakes demonstrate the adaptability of the elongate, limbless body plan by effectively navigating habitats throughout the world (Gans 1986). The most general gait used by limbless organisms is lateral undulation, in which body bends primarily in the plane of the substrate are passed from head to tail. When backward slipping of these bends is prevented by terrain heterogeneities, the resulting forces propel the snake forward (Mosauer 1932). While undulatory locomotion in fluids has been well-studied (Fish and Lauder 2006; Childress et al. 2012; Rodenborn et al. 2013), less is known about undulatory motion in terrestrial habitats.

We endeavored to identify strategies for undulatory locomotion in terrestrial terrain by comparing two species adapted to different habitats. The sand-specialist shovel-nosed snake *Chionactis occipitalis* (Recent genetic testing indicates the genus *Chionactis* is a sub-genus of *Sonora* such that *C. occipitalis* is synonymous with *Sonora occipitalis* [Cox et al. 2018]. As in both our previous work and the majority of previous literature on this species refers to it as *C. occipitalis* we will do so here) (Fig. 1a) and the habitat generalist, the corn snake *Pantherophis guttatus* (Fig. 1b). In this article, we use the terms specialist and generalist to refer to the types of terrains the snakes typically encounter in their natural habitats. *Pantherophis guttatus* is a

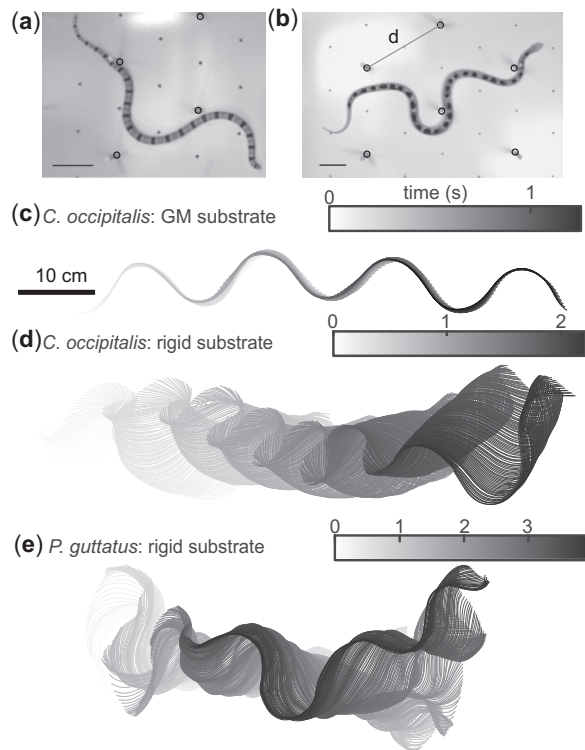


Fig. 1 Sand-specialist *C. occipitalis* and habitat generalist *P. guttatus* moving on model terrain in the lab. Scale bars in the lower left corner of (a) and (b) are 10 cm. (a) *Chionactis occipitalis* in a 12 cm lattice. The 12 and 16 cm spacings were achieved by removing posts from the 6 and 8 cm lattices, respectively. Post base locations are circled. The dark points are the remaining holes. (b) *Pantherophis guttatus* in a 16 cm lattice. Lattice spacing, d , as shown. Black dots painted on the midline were used for tracking. (c) Tracked midlines of the sand-specialist moving on a model granular material (GM), $296 \pm 40 \mu\text{m}$ diameter glass particles. All midlines collected through the trial are shown, colored by time. Scale bar is the same for (d) and (e). (d) *Chionactis occipitalis* and (e) *P. guttatus* moving on the rigid, low-friction substrate. All snakes moving from left to right.

semi-arboreal habitat generalist; its range covers an area that consists of a variety of terrains such as wetlands, forests, and man-manipulated areas. In contrast, *C. occipitalis* lives in a desert environment and is typically confined to loose, dry sand. While there are a number of gaits these snakes can perform, in this study, we focused on lateral undulation. We note that, in the experimental terrains we used in this study, the snakes always used lateral undulation and we did not observe other gaits.

Lateral undulation relies on the use of “push-points” in the surroundings to resist slipping of the body thus generating propulsion. These push-points may be discrete obstacles (Gray and Lissmann 1950; Kelley et al. 1997), heterogeneities introduced to a yielding substrate by the motion of the trunk (e.g., piles of sand; Schiebel et al. 2019), frictional

anisotropy of the ventral scutes (Hu et al. 2009), or some combination of these modes. The kinematics of generalist snakes using lateral undulation to traverse a simplified model of terrestrial terrain heterogeneities—posts embedded in a rigid substrate—varied as a function of the density of the model push-points (e.g., Bennet et al. 1974; Kelley et al. 1997). As a counterpoint, *C. occipitalis* used a stereotyped waveform to move across granular matter (GM) like the sand of its desert habitat (Mosauer 1933; e.g., Fig. 1c). We discovered that this specific waveform is beneficial for movement on GM substrates, rationalizing its conserved appearance across individuals of this species (Schiebel et al. 2019).

We elected to use as a model terrain a low-friction whiteboard substrate with regular arrays of posts. While the snakes could make some progress across the low-friction surface via the frictional anisotropy of the ventral scutes (Hu et al. 2009; Supplementary Movie S1), the body experienced high lateral slipping (Fig. 1d and e, Supplementary Movie S1). Our aim was to create an assay in which the animal would move more effectively if it used the discrete heterogeneities as push-points as opposed to relying on forces generated using the substrate alone. We expected the generalist, which often uses discrete push-points in its natural habitat, to more proficiently use the posts to traverse the arena. We hypothesized the specialist, which in nature has access to a continuous sand substrate that allows the snake to generate push-points at will, would not be as adept at using the posts for propulsion. In using this model, our intent was to challenge the animals’ locomotor capabilities and observe how they chose to self-deform in response. By comparing similarities and differences in waveform and performance, we hoped to tease apart differences in behavioral strategy between animals adapted to move using different terrains.

Insight into the benefits and limitations of different locomotor strategies can both provide a basis for future exploration of control in undulatory locomotion as well as inspiration for locomotor strategies for use in snake-like robots.

Methods

To affix the posts, we drilled holes in the whiteboard which held small wooden dowels using an interference fit (see Fig. 1a and b). The 3D printed sleeves were then placed over the dowels. For this work, we used cylindrical posts 0.64 cm in diameter, but the system was designed so that arbitrary shapes could be printed and put onto the lattice. Lattice

Table 1 Lengths of individuals used

Animal no.	Length (cm)	Mass (g)
120	36.4	20
122	39.2	21
123	40.1	20
21	57.9	57
22	58.1	60

Numbers 21 and 22 are *P. guttatus*, all others are *C. occipitalis*.

configurations were hexagonal, such that each post was equidistant to its nearest neighbors. We varied lattice spacing, d , the nearest-neighbor distance between posts (Fig. 1b).

The lattices were placed on top of the GM in the fluidized bed used in our previous work (Schiebel et al. 2019). This served to both ensure the lattice was level, as after fluidization the GM is level with respect to gravity, as well as provide an inescapable arena and a rigid structure to mount the camera.

We tested three wild-caught *C. occipitalis* (Appendix 1) on the homogeneous whiteboard and in six lattice spacings ($d = 4, 6, 7, 8, 9$, and 12 cm) and collected a minimum of three runs per individual for each treatment. The videos were digitized by tracking the animal's natural black bands using MATLAB and the tracking algorithm described in Sharpe et al. (2015). We acquired two juvenile, albino *P. guttatus* through the pet trade. The experimental procedures were the same as those for *C. occipitalis* with the exception that black marks were painted along the midline of *P. guttatus* to facilitate tracking (see Fig. 1b). As the *P. guttatus* were longer than *C. occipitalis* (Table 1), we tested them in the larger lattice spacings ($d = 6, 7, 9, 12$, and 16 cm). To facilitate comparison between the species, we defined post spacing as d/L , where L is the total body length.

We chose lattice spacings that were large enough that the animal had flexibility in choosing its waveform. We tested *C. occipitalis* in a 2 cm lattice as well, but at this spacing the distance between posts was only slightly wider than the snake body and the waveform were qualitatively different from that at all the other spacings (Supplementary Fig. S1). Thus, we used $d = 4$ cm as the smallest spacing for the specialist, and the comparable $d = 6$ cm for the generalist. As the largest spacing, we used $d = 12$ and 16 cm. At this spacing the snakes are long enough they could physically reach three posts simultaneously.

While in the future, we would like to include more *P. guttatus* individuals in our study, we note that the behavior and performance of the two snakes tested were comparable. Further, their movement

through the lattices was similar to that of another generalist tested in the same terrain, the eastern garter snake *Thamnophis sirtalis sirtalis* (PES, personal observation).

We also challenged the animals to ascend the lattice on an incline. We used the tilting functionality of the arena to incline the whiteboard and lattices used in the level ground trials (0°) to three different slopes, 15.5, 20, and 30 deg (± 1 deg). The arena was mounted on an axle held by rotational ball bearings, and two linear motors (Firgelli) mounted at one end controlled the angle. The axle was located between the midpoint of the bed and the end opposite the actuators. This design kept the inside of the arena low enough to be accessible to the researcher even when tilted, while ensuring that the stable position of the bed was resting in the level position such that if the motors were to fail it would fall back onto the supporting frame.

We were interested in studying how the animals would interact with the surroundings if their goal was to move as quickly as possible. Thus, in all trials, we elicited an escape response. We assumed that in this case the snakes' goal was to move away from the stimulus. In some cases, this simply required releasing the animal, in others light tail taps were used (see Appendix 1 for more detail). We had to use tail tapping more frequently to motivate *Pantherophis*. In some instances, the snakes were startled by the taps (see Supplementary Movie S3), although this did not occur with every tap nor in every trial. As the kinematic changes when startled were small compared to the overall waveform we do not believe they impacted the results of the analysis.

A trial was included if the snake met the "successful stop condition" by traversing roughly 80% of the arena or more before electing to stop moving or contacting a sidewall. The exception to these criteria was treatments where the animal may not make appreciable progress—the whiteboard without lattices and ascending the largest spacing inclined lattices. In this case, we used the "failure stop condition"; after approximately five undulations the animal was permitted to continue moving until electing to stop or, in the incline trials, sliding out of the lattice.

Results and discussion

Species-dependent kinematics

Both species were able to traverse the arena when posts were present at all spacings tested (Fig. 2). We observed lateral slipping of body segments which was curtailed by contact with the posts (Fig. 2). The

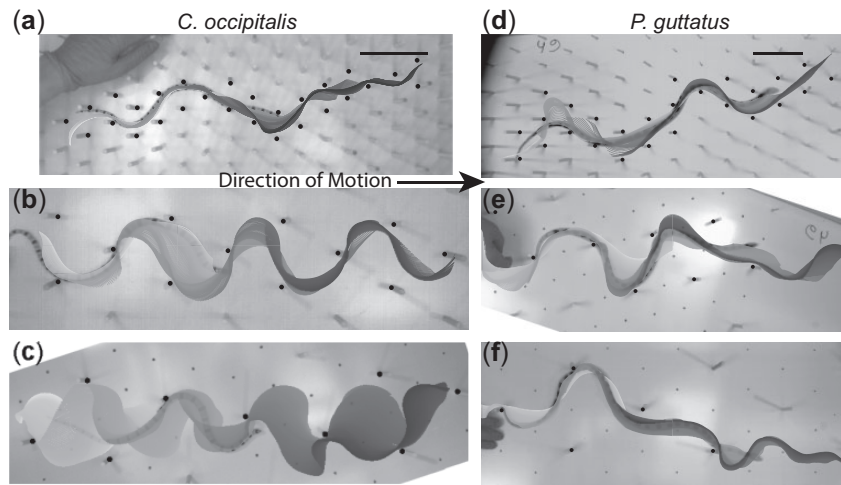


Fig. 2 Traces of snake kinematics in different lattices. Snake midlines at each moment are plotted with color according to time from beginning (white) to end (black) of the trial. Black circles have been added to highlight the posts nearest the body. Arrow indicates the direction of motion of all panels. A 10 cm scale bar in (a) and (d) applies to (b, c) and (e, f), respectively. (a–c) *Chionactis occipitalis*. (d–f) *Pantherophis guttatus*. (a) $d = 4$ cm, $d/L = 0.11$. (b) $d = 8$ cm, $d/L = 0.21$ (c) $d = 12$ cm, $d/L = 0.32$ (d) $d = 6$ cm, $d/L = 0.10$ (e) $d = 12$ cm, $d/L = 0.21$ (f) $d = 16$ cm, $d/L = 0.28$.

generalist gave an overall impression of greater competence, and we observed simultaneous slipping of the entire body more frequently in the sand-specialist snake as compared to the generalist (Supplementary Movie S2). We hypothesized this was a result of the waveforms used by the animals.

Chionactis occipitalis often used regular, sine-like waveforms, especially as lattice spacing increased (e.g., Fig. 2a–c). We also find that *C. occipitalis* predominantly used its sand-swimming wavelike shape when moving on the whiteboard with a single embedded post, even once it contacted the post and thus presumably had “knowledge” of its existence (personal observation).

In contrast, *P. guttatus* displayed a greater variety of wave shapes. The generalist would simultaneously use high-curvature bends taking up only a small fraction of the trunk and long, low-curvature sections (e.g., Fig. 2d–f). Future study could expand the lattice spacings to elucidate whether these observations hold true at spacings larger than those tested here as well as the transition from forward progress when posts are present at a high enough density to the high-slip motion on the whiteboard without obstacles (compare Fig. 1e with Fig. 2f).

The waves of undulation were primarily in the horizontal plane. While snakes may superimpose a vertical wave of smaller amplitude relative to the horizontal wave to improve performance (Hu et al. 2009; Schiebel et al. 2019a), thrust is generated primarily by the action of the horizontal wave. Thus, we chose to focus this study on kinematics in this plane. We captured snake kinematics using curvature

along the body as a function of arclength along the midline, s , and time, t . We characterized the waveforms using the average number of waves on the body, ξ (Fig. 3a; Sharpe et al. 2015), and the maximum curvature on the body, κ_m , normalized by the total snake length (κ_{mL}) (Fig. 3b). We used κ_{mL} to allow for comparison between the species of different average length. For example, if one were to take a snapshot of a snake and double the height and width, κ_m will decrease by a factor of two while κ_{mL} will stay the same.

ξ was obtained by dividing the total length of the snake by the average arclength of the body waves, $\bar{\lambda}_s$. We first calculated $\bar{\lambda}_s/2$ by measuring the arclength between points of zero curvature on the body then doubled and averaged these values to obtain the average, $\bar{\lambda}_s$. The wavenumber was thus $\xi = L/\bar{\lambda}_s$. κ_{mL} was calculated by finding the maximum curvature at each frame and multiplying by snake length.

We collected waveform parameter values for all individuals and lattice spacings and compared the distribution for *C. occipitalis* and *P. guttatus*. The distribution of both ξ and κ_{mL} was more sharply peaked in *C. occipitalis* (Fig. 3 solid black curves) than in *P. guttatus* (Fig. 3 dashed gray curves). This was in accord with our observation that the generalist snakes used a wider variety of wavelike shapes when traversing the arrays.

We previously discovered that, when confronted with a single row of posts embedded in a substrate that the snakes could move across like the GM in their natural habitat, *C. occipitalis* adhered to its specialized sand-swimming waveform even when

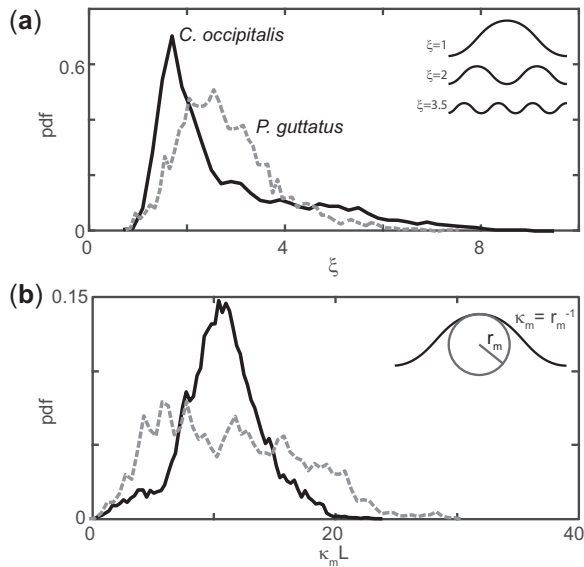


Fig. 3 Distribution of waveform parameters. Data from all individuals and lattice spacings combined. (a) Distribution of wavenumber, ζ . Inset shows an example of a waveform with constant κ_{mL} and different ζ . Black and gray curves are for *C. occipitalis* and *P. guttatus*, respectively. (b) Distribution of normalized maximum curvature, κ_{mL} . Color as in (a). Inset shows the definition of κ_m .

traversing the array (Schiebel et al. 2019). We hypothesized that the specialist used a similar strategy even in the rigid lattices without a GM substrate.

Principal component analysis

Inspired by work on the nematode *C. elegans* (Stephens et al. 2008), we used principal component analysis (PCA) to search for a low-dimensional representations of each species' waveform. We characterized the snake postures using curvature times the body length, $\kappa(s, t)L$, at each moment in time as a function of arclength from neck to vent. To find the principal components (PCs), we combined all of the curvatures from each species and calculated the eigenvectors of the curvature covariance matrix. The resulting eigenvectors, the PCs, form an orthogonal basis for the variation of κ along the body.

Given our previous results, in which we found the waveform used by the sand-specialist on yielding substrates was well-described by two PCs (Schiebel et al. 2019a, 2019b), we calculated the first two PCs, $PC_1(s)$ and $PC_2(s)$, and their associated coefficients $(\kappa_m L)_1(t)$ and $(\kappa_m L)_2(t)$, where

$$\kappa L(s, t) \approx (\kappa_m L)_1(t)PC_1(s) + (\kappa_m L)_2(t)PC_2(s). \quad (1)$$

PC_1 and PC_2 of the sand-specialists on sand were well-described by a sine and a cosine (Schiebel et al. 2019). The PCs calculated using data from *C. occipitalis* on the rigid substrate in the lattices were

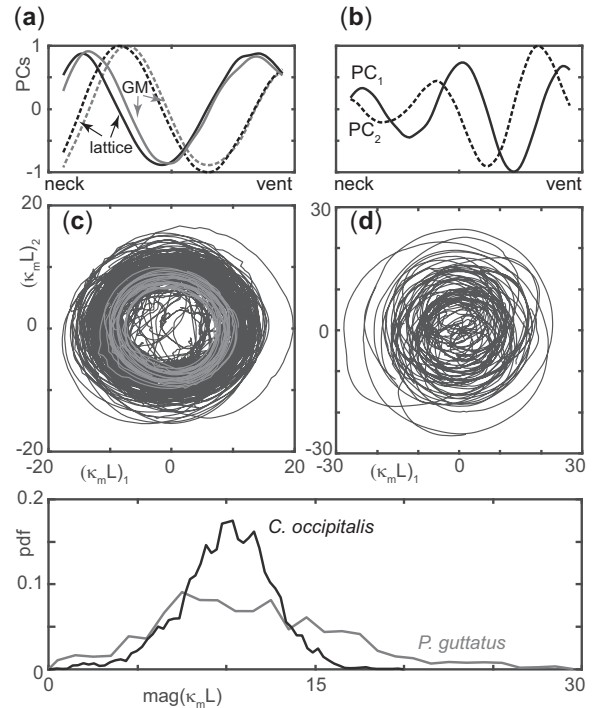


Fig. 4 PCA of snake kinematics. PCs are normalized by the maximum value occurring in the PCs from one dataset. (a) PC_1 (solid lines) and PC_2 (dashed lines) of κL for *C. occipitalis* on GM (gray curves, 3 individuals, 9 trials) and in the arrays (black curves, 3 individuals, 56 trials). (b) PC_1 (solid line) and PC_2 (dashed line) of κL for *P. guttatus* in the arrays (2 individuals, 39 trials). (c) Coefficients associated with *C. occipitalis* PCs shown in (a). The trajectory through the $(\kappa_m L)_1$, $(\kappa_m L)_2$ space calculated using the GM PCs and data for the specialist on GM is shown in gray, and that for the lattice PCs and data is shown in black. (d) Coefficients associated with *P. guttatus* PCs shown in (b). The axis range is larger than (c), consistent with the larger κ_{mL} measured on the generalist (Fig. 3b). (e) Histogram of the radial distance from the origin of each $(\kappa_m L)_1$, $(\kappa_m L)_2$ pair.

$\text{mag}(\kappa_m L) = \sqrt{(\kappa_m L)_1^2 + (\kappa_m L)_2^2}$. Black curve is *C. occipitalis*, calculated using the whiteboard data shown in (c) (excluding the GM data shown in gray). Gray curve is *P. guttatus* calculated using the data shown in (d). Histograms include 20,169 specialist and 12,111 generalist data points. Note that in (c–e) no one animal or trial dominated any part of the plot (see Supplementary Fig. S2).

comparable to those on homogeneous GM with no lattice (Fig. 4a black versus gray curves). The generalist PCs were two sine and cosine-like waves, but, unlike the specialist, the amplitude increased posteriorly from head to tail (Fig. 4b).

The amount of variance captured by the first two PCs represents how accurately we can reconstruct the original data. For *C. occipitalis* moving across the surface of homogeneous GM, the first two PCs captured 91.5% of the variance; these PCs represented most of the shapes made by the snake. In the arrays, the first two *C. occipitalis* PCs captured

70%. In contrast, the first two PCs calculated using the generalist in the arrays only accounted for 40.8% of the variance. This likely reflects the greater variation in the generalist's waveforms.

On homogeneous GM, the coefficients $(\kappa_m L)_1$ and $(\kappa_m L)_2$ associated with the specialist's PCs traced a circle of approximately constant radius through time (Fig. 4c gray curves). Circular trajectories like these correspond to a traveling wave of constant amplitude. Similarly, $(\kappa_m L)_1$ and $(\kappa_m L)_2$ calculated using data from *C. occipitalis* traversing the arrays also followed circular trajectories (Fig. 4c black curves).

The radius of the circle was more variable than that calculated from data on the homogeneous GM. We conjecture this is because, especially in the smaller lattice spacings, the snakes can modulate the waveform (e.g., Fig. 2a). Since the coefficients are rarely zero, we posit that the sand-swimming waveform is always present on the body, but it may be modulated by higher-order PCs when moving in the arrays (Fig. 4e).

The generalist coefficients indicated these PCs were at times present on the body and creating a traveling wave. However, the distance from the origin, $\text{mag}(\kappa_m L)$, varied more widely than in the specialist, consistent with the wider range of $\kappa_m L$ measured in the *P. guttatus* data (Fig. 3b vs. Fig. 4e). There were also data points near the origin, which indicated that the waveform generated by these first two waveshapes was not always clearly present on the body. To quantify how often the coefficients were near the origin, we calculated what percent of all the data points collected had $\text{mag}(\kappa_m L) < 1$. In the specialist, 0.07% of the $\text{mag}(\kappa_m L)$ was less than one compared to 9.6% for the generalist. We note that for both species the path traced out by the coefficients through time varied smoothly through each trial.

These results supported our hypothesis that the sand-specialist snake used its stereotyped sand-swimming waveform even when no GM substrate was present. PCA also indicated that the generalist snakes did not have an equivalent low-dimensional waveform.

Strategy and performance

We next hypothesized that the greater variety in the generalist waveforms was an adaptation to contending with the variety of terrains in their natural habitat and thus *P. guttatus* would outperform the sand-specialist in the model terrain.

We characterized performance using the average slip angle, $\bar{\beta}_s$. $\bar{\beta}_s$ is zero if every segment on the body follows exactly the path of its anterior

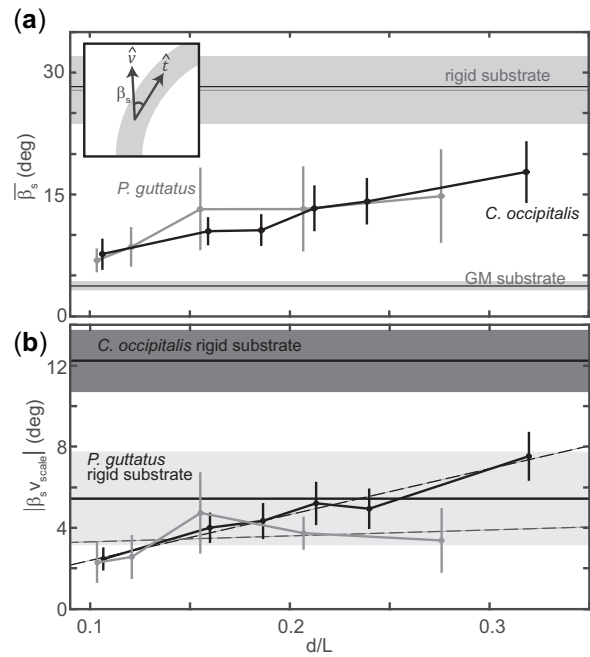


Fig. 5 Slip versus lattice spacing d/L for *C. occipitalis* and *P. guttatus*. d/L calculated using the average length for the species. (a) Average and standard deviation of the average slip angle for all individuals and trials at each lattice spacing are shown for *C. occipitalis* (black markers and lines) and *P. guttatus* (gray markers and lines). Horizontal lines denote slip on the substrate without any posts. Shown are the values for *C. occipitalis* (black line) and *P. guttatus* (gray line) on the rigid substrate and *C. occipitalis* on GM, as labeled. Rectangular patch denotes the standard deviation. The values for both species on the substrate were similar so the patch shown encompasses the area covered by the standard deviation of both species. (inset) Diagram of β_s . Gray curve illustrates the snake body with example local tangent and velocity unit vectors \hat{t} and \hat{v} . (b) Scaled slip versus d/L . Line colors consistent with (a). The habitat generalist homogeneous substrate performance was different when measured with this metric, thus the mean (horizontal line) and standard deviation of the means (light gray patch) are shown separately from *C. occipitalis* (black line and dark gray patch). Dashed gray and black lines are linear fits to the generalist and specialist data, respectively. Generalist slope = 2.9 and $R^2 = 0.04$. Specialist slope = 22.6 and $R^2 = 0.96$.

neighbor, as if the snake were in a tube. β_s is the unsigned angle between the local velocity and tangent unit vectors, $\beta_s(s, t) = |\hat{v}(s, t) \cdot \hat{p}\hat{t}(s, t)|$ (Fig. 5). $\bar{\beta}_s$ is the average of β_s over all segments and times. We chose this metric to facilitate comparison between the species because β_s is independent of snake length and calculated from local information. Thus it avoids the ambiguity of calculating variables like wavelength on the generalist waveforms, which may have several waves of different wavelengths on the body simultaneously.

Contrary to our expectations, the slip of both species was similar (Fig. 5a). Both species experienced

similar, large slip when on the homogeneous whiteboard (Fig. 5a, horizontal lines). Adding the lattice to the whiteboard resulted in decreased β_s relative to the substrate alone for both species (Fig. 5a, curves). $\bar{\beta}_s$ was dependent on lattice spacing on the whiteboard; as spacing between the posts increased the slip angle increased. This result was intuitive; the limit $d \rightarrow \infty$ is the homogeneous substrate. Future studies using even larger spacings can determine if the performance quantified using slip monotonically degrades to the homogeneous case.

We observed two sources of slip. *Pantherophis guttatus* would slide local sections of the body perpendicular to the overall direction of motion, causing large β_s . For example, the snake's head would slide around a post to "grab" onto the obstacle or the tail would swing across the substrate when not in contact with a post. This slipping could occur while other sections of the body were either moving smoothly forward or static relative to the substrate and thus did not appear to negatively impact the ability of the snake to make effective forward progress. The other source of slip was more often observed in *C. occipitalis*. Especially as post spacing increased, simultaneous slipping of the entire body could be observed, leading to locomotion like that on the homogeneous whiteboard (see Fig. 1d versus Fig. 2c; Supplementary Movie S2).

A drawback of the slip measure was that it depended only on the velocity unit vector. Thus, sections of the body that were moving very little relative to the substrate could be dominated by noise and contribute large values to the mean that did not accurately represent how much the body is slipping. Thus, we scaled the slip values using the local velocity magnitudes. For each trial, we calculated the velocity magnitude of each segment at all times. We then divided this array by the maximum value. The resulting array, v_{scale} , ranged from small values where the body segments were moving slowly to numbers close to unity where the body was moving near the maximum observed speed. We multiplied the slip array by this scaling array then averaged over space and time. The resulting $|\beta_s v_{scale}|$ provided a slip metric that more heavily weighted the contributions of fast-moving segments.

The performance on the homogeneous substrate described using $|\beta_s v_{scale}|$ was different for the two species (Fig. 5b, horizontal lines). The habitat generalist moved with less scaled slip relative to the specialist as the lattice spacing increased. *Chionactis occipitalis* slip increased linearly with lattice spacing (Fig. 5b, black dashed line $R^2 = 0.96$), while *P.*

guttatus slip was not strongly correlated with spacing (Fig. 5b, gray dashed line $R^2 = 0.04$).

The performance of the generalist was similar to the homogeneous substrate with and without the posts. We found that, while the specialist would continue performing their preferred waveform on the whiteboard, the generalist appeared to purposefully plant sections of the body that facilitated movement (Supplementary Movie S1).

While the species' kinematics differed, our results indicated that both strategies were successful at moving through our model terrain; all snakes were able to traverse the lattice until reaching the "successful stop condition." Further, performance characterized using the slip metric was similar for both species, although scaled slip revealed a modest difference in performance.

The low-friction substrate was challenging because the animals experienced high-slip unless they generate appropriate normal forces using the discrete obstacles. However, the substrate also did not penalize unneeded slipping of the body. Therefore, we further challenged the snakes by placing the lattice on an incline and chasing the snakes up against gravity.

Ascending slopes

We expected that the habitat generalist strategy would be more effective than the specialist strategy as the terrain incline increased. On level ground, failing to coordinate appropriate propulsive forces would result in the animal slipping in place but not losing progress. When moving against gravity, however, without sufficient propulsion the animal would lose progress by slipping down the slope.

Similar to our observations on level ground, *P. guttatus* would bend the body and "grab" a post then maintain consistent contact as it ascended (Fig. 7). In contrast, *C. occipitalis* would make and break contacts, sometimes even sliding backward down the incline (Fig. 6).

For example, at time $t=0$ s in Fig. 6, the *C. occipitalis* was touching two posts, highlighted by the circle and square (note all posts were cylindrical, the square is intended only to orient the reader). While the snake appeared to grab the "circle" post at $t=0$ s, by $t=0.63$ s it had completely lost contact with the "circle" post and slid down the incline until colliding with the square-marked post. Using the "square" post it was able to make some progress uphill (see $t=2.25$ s). However, at $t=3.5$ s, we see the body rotating off of the "square" post as it did

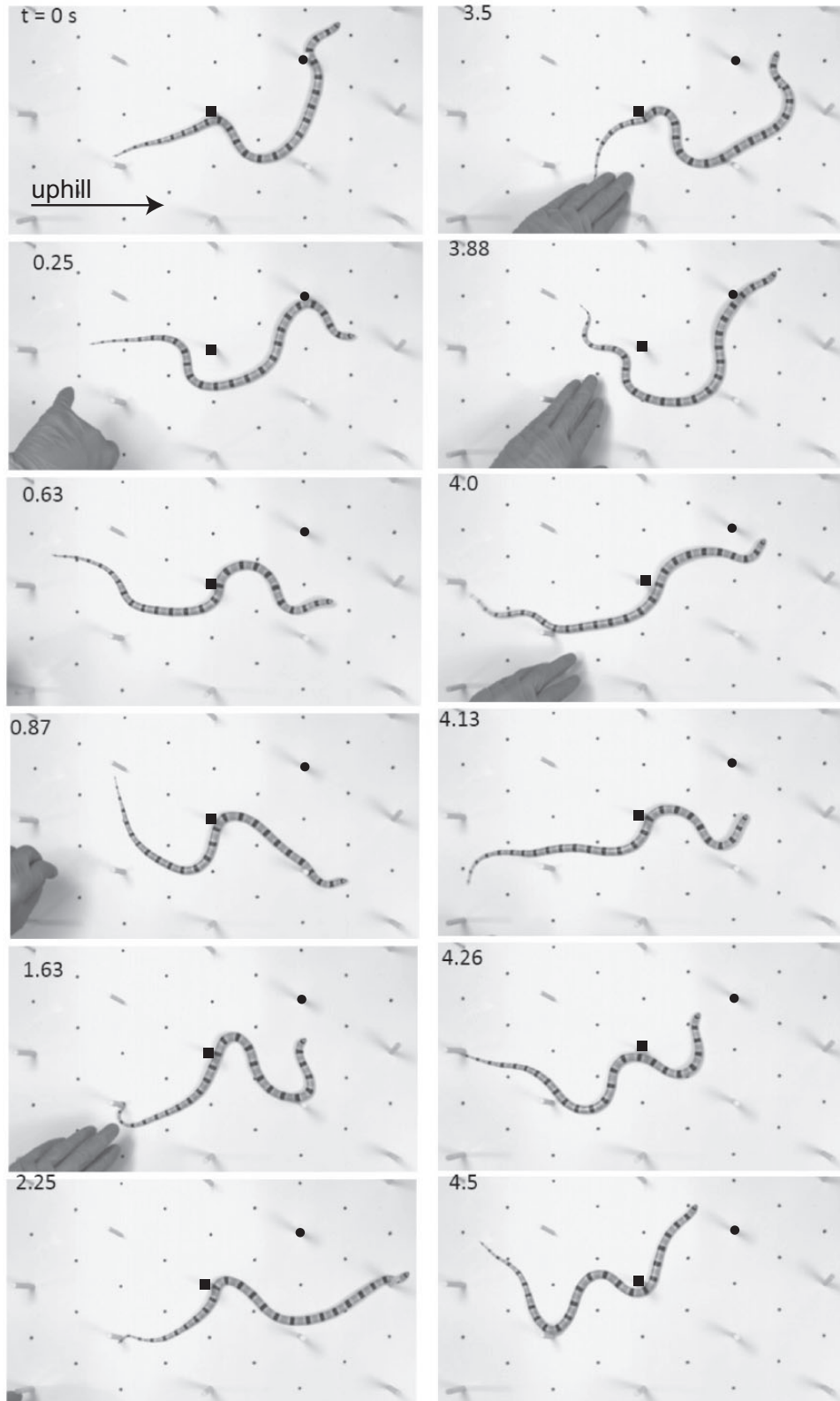


Fig. 6 Sand-specialist *C. occipitalis* ascending 20° incline. $d/L = 0.32$.

with the circle-labeled post at $t = 0.25$ s, and by $t = 3.88$ s the snake again completely lost contact with the “square” post and, despite a transient

contact with the “circle” post, again loses progress by sliding down the hill. This behavior, in which the snakes used a post to ascend the hill for some time

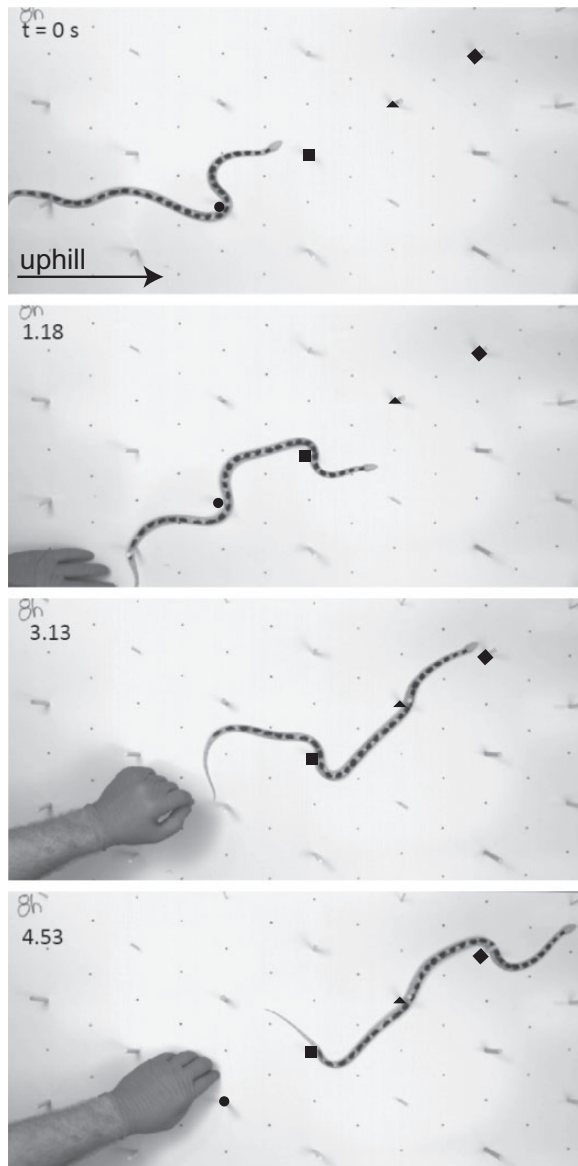


Fig. 7 Habitat generalist *P. guttatus* ascending 30° incline. $d/L = 0.28$.

only to lose contact and progress, was common in *C. occipitalis* (see also [Supplementary Movie S3](#)).

In comparison, *P. guttatus* was able to make and maintain contacts with the posts. It was not uncommon for a snake to use a single post from the time it grabbed on near its head until the post reached the tail (e.g., the square-labeled post in [Fig. 7](#)). The generalist snakes were able to always maintain appropriate forces to prevent falling down the incline ([Supplementary Movie S3](#)).

This locomotor task penalized insufficient propulsive forces, as opposed to the level ground task where snakes would not lose progress if they failed to maintain contacts. When faced with this terrain,

the stereotyped waveshape used by the specialist was not as effective as the more variable generalist kinematics. Unlike in the level ground trials where the snakes were always able to traverse the terrain, in all three of the incline trials taken in the 12 cm spacing lattice at a slope of 20° or 30° degrees the specialist either made no forward progress or slid backward down the slope. The generalist, however, never lost progress sliding down the hill.

It is noteworthy that the specialist snake was capable of using other strategies. For example, in a highly confined lattice ($d = 2$ cm), the waveforms were visibly changed, characterized by straight sections and local, high-curvature bends more like the shapes of the generalist than the specialist on sand ([Supplementary Fig. S1](#)). We also observed the snakes grabbing onto posts with the tail. Although this behavior did not appear in the majority of trials, both [Supplementary Movies S2](#) and [S3](#) have examples of the tail grabbing behavior. In [Supplementary Movie S3](#), while the tail is wrapped around a post the anterior portion performs several ineffectual undulations. We think this is particularly interesting as it demonstrates that while these animals are capable of varying their self-deformation pattern, they still frequently default to the preferred sand specialized waveform.

Conclusion

By propagating waves of body bending from head to tail, limbless organisms like snakes can traverse terrain composed of rocks, foliage, soil, and sand. Previous research elucidated how snakes use body bends to interact with heterogeneities in the surroundings to generate propulsive forces. In this work, we compared the kinematics and performance of two snake species, a habitat generalist and a sand-specialist, traversing hexagonal arrays of posts on a slippery substrate. By comparing species adapted to different habitats, we identified different strategies for traversing complex terrestrial terrain. We found that the generalist *P. guttatus* used a broader variety of waveforms in traversing the arrays than the sand-specialist *C. occipitalis*. The specialist largely adhered to a stereotyped waveform previously found to be beneficial during movement on the surface of yielding, hysteretic material like the sand of its natural habitat. On level ground, both species moved with the same amount of slip and both were able to traverse the arena. Upon introducing an incline, however, the generalist was still able to cross the arena in all treatments while the specialist failed to progress at the highest slope/largest spacing combinations.

These results indicate that both of these kinematic strategies are effective during locomotion in terrestrial terrains where there are discrete obstacles that can be used as push-points. The sand-specialist strategy, which uses an omnipresent, stereotyped waveform, may be useful as a simple control of snake-like robots. However, a more variable waveform like that used by the generalist, which we hypothesize is controlling its waveform in response to environmental forces rather than targeting desired kinematics, may be necessary during more challenging tasks like moving uphill.

The difference in kinematics and performance of these two species suggests that the animal's neuromechanical systems may be specialized for movement in their natural habitat. Thus, while the sand-specialist was physiologically capable of adopting more complicated waveforms, it most frequently reverted to its preferred waveform for movement on the sand of its desert habitat. This study indicates the lateral undulation used in different terrain types may be different gaits that evolved in response to the physics of the animal's surroundings (see [Jayne 2020](#) for relevant discussion of snake gaits).

In this article, we used PCA to search for waveforms that were well-described by two PCs. Future work could explore whether the generalist does have preferred kinematics, analogous to the sand-swimming waveform, which exists in a higher-dimensional space. We also propose that comparing the kinematics of the snakes in greater detail may provide insight into their control strategies. We previously made progress understanding the control strategy of the sand-specialist by observing its kinematics as it interacted with multi-component terrain. By comparing how species adapted to move in different habitats self-deform in response to the same terrain it may be possible to glean the types of environmental information the snakes are using and how they incorporate that information in choosing and executing a waveform.

Acknowledgments

We thank Kevin and April Young for collecting the *C. occipitalis* and Mark Lowder for his assistance in creating the non-sand-specialist tracking code. We thank the reviewers for their input which improved the quality of the article.

Funding

This work was supported by NSF PoLS PHY-1205878, PHY-1150760, and CMMI-1361778. ARO W911NF-11-1-0514, NDSEG 32 CFR 168a (P.E.S.),

and the NSF Simons Southeast Center for Mathematics and Biology.

Data availability statement

Data available at SMARTech repository.

Supplementary data

[Supplementary Data](#) available at *ICB* online.

References

- Bennet S, McConnell T, Trubatch SL. 1974. Quantitative analysis of the speed of snakes as a function of peg spacing. *J Exp Biol* 60:161–5.
- Childress S, Hosoi A, Schultz WW, Wang J, (eds.). 2012. Natural locomotion in fluids and on surfaces: swimming, flying, and sliding. Vol. 155. New York: Springer Science & Business Media.
- Cox CL, Davis Rabosky AR, Holmes IA, Reyes-Velasco J, Roelke CE, Smith EN, Flores-Villela O, McGuire JA, Campbell JA. 2018. Synopsis and taxonomic revision of three genera in the snake tribe sonorini. *J Nat Hist* 52:945–88.
- Fish FE, Lauder GV. 2006. Passive and active flow control by swimming fishes and mammals. *Annu Rev Fluid Mech* 38:193–224.
- Gans C. 1986. Locomotion of limbless vertebrates: pattern and evolution. *Herpetologica* 42:33–46.
- Gray J, Lissmann HW. 1950. The kinetics of locomotion of the grass-snake. *J Exp Biol* 26:354–67.
- Hu DL, Nirody J, Scott T, Shelley MJ. 2009. The mechanics of slithering locomotion. *Proc Natl Acad Sci U S A* 106:10081–5.
- Jayne BC. 2020. What defines different modes of snake locomotion?. *Integr Comp Biol* 60:156–70.
- Kelley KC, Arnold SJ, Gladstone J. 1997. The effects of substrate and vertebral number on locomotion in the garter snake *thamnophis elegans*. *Funct Ecol* 11:189–10.
- Mosauer W. 1932. On the locomotion of snakes. *Science* 76:583–5.
- Mosauer W. 1933. Locomotion and diurnal range of *Sonora occipitalis*, *crotalus cerastes*, and *crotalus atrox* as seen from their tracks. *Copeia* 1933:14–6.
- Rodenborn B, Chen C-H, Swinney HL, Liu B, Zhang HP. 2013. Propulsion of microorganisms by a helical flagellum. *Proc Natl Acad Sci U S A* 110:E338–47.
- Schiebel PE, Astley HC, Rieser JM, Agarwal S, Hubicki C, Hubbard AM, Cruz K, Mendelson J, Kamrin K, Goldman DI. 2019a. Mitigating memory effects during undulatory locomotion on hysteretic materials. [bioRxiv748186](#).
- Schiebel PE, Rieser JM, Hubbard AM, Chen L, Zeb Rocklin D, Goldman DI. 2019b. Mechanical diffraction reveals the role of passive dynamics in a slithering snake. *Proc Natl Acad Sci U S A* 116:4798–803.
- Sharpe SS, Koehler SA, Kuckuk RM, Serrano M, Vela PA, Mendelson J, Goldman DI. 2015. Locomotor benefits of being a slender and slick sand swimmer. *J Exp Bio* 218:440–50.
- Stephens GJ, Johnson-Kerner B, Bialek W, Ryu WS. 2008. Dimensionality and dynamics in the behavior of *c. elegans*. *PLoS Comput Biol* 4:e1000028.

Appendix 1

Animal experiments

Chionactis occipitalis was collected by Kevin and April Young in the Colorado Desert near Yuma, Arizona, USA under scientific collection permits (SP790952, SP625775, SP666119) approved by the Arizona Game and Fish Department and held in the Physiological Research Laboratory at Georgia Tech. *Pantherophis guttatus* were acquired through the pet trade. Neither the sex nor the age of the animals was determined; gender and age dependent effects were beyond the scope of this study. All experimental procedures were conducted in accordance with the Georgia Institute of Technology IACUC protocols A14066 and A14067.

The temperature in the trackway and snake holding area was measured prior to each trial. Lamps were used to ensure the temperature in both remained at $26^{\circ}\text{C} \pm 1^{\circ}\text{C}$. The heat lamps on the trackway were turned off during data collection and LED lights were used for illumination.

Each day the individuals to be tested were transported from the housing facility to the laboratory

where we conducted the trials. Snakes that were in the process of shedding were not used. During a trial, the snake was removed from its holding container and placed immediately in the fluidized trackway. The *C. occipitalis* tended to be skittish and handling both during trials and in the housing facility was kept to a minimum. The animals would often immediately flee across the surface upon introduction to the trackway; otherwise, a light tail tap would elicit an escape response. If an individual did not respond to this stimulus they were returned to the holding container. *Pantherophis guttatus* was less easily startled. These animals were first encouraged to move via constant, gentle tail taps outside of the arena. Once the animal was moving away from this stimulus (rather than ignoring or displaying defensive behaviors), it was introduced to the arena and encouraged with tail taps using a soft, white pipe cleaner that would not impact the tracking. If an individual failed to perform for three trials in a row they would be retired from the day's studies. Snakes were tested at most every other day with a maximum of two successful trials collected per day.